EXPERIMENTAL STUDY ON LIQUEFACTION OF SANDY SOIL ON COHESIVE LAYER

by
Yukitake Shioi[I]

SYNOPSIS

With regard to the liquefaction of saturated sandy soils during an earthquake, the influence of clayey soils existing below sandy soils was examined by vibration experiments with models. As a result, it was found that the existence of a clayey layer below greatly affected liquefaction. Models used were 9 models for soils and 2 models for piles. The experiments gave qualitatively satisfactory results, but left quantitative evaluation as a future problem.

METHOD OF EXPERIMENT

Many researches have been made so far on the liquefaction of saturated sandy soils. Generally in many points among the places where liquefaction has taken place during earthquake, it is found that cohesives soils very ductile are distributed below the liquefied sandy soils (Fig. 1). In order to examine the influence of these cohesive soils below a sandy layer, vibration tests were made, by using the six kinds of models shown in Fig. 2. Model 1, 2, 3, 4, 5 and 6 were respectively prepared to examine the dynamic property of cohesive soil, the influence of the weight of the sandy layer, the effect of constraining the layer above cohesive soil, the dynamic properties in case of dry sand, the vibration properties of saturated sand on cohesive soils and the influence of an impermeable surface layer on a saturated sandy layer.

Then, the three kinds of models shown in Fig. 3 were used to check the influence of the thickness of sand. To know the behaviour of the piles put in the soils of Models 5 and 6, two models as shown in Fig. 4 were prepared.

The arrangement of measuring apparatus in the models of Fig. 2 is shown in Fig. 5. The shaking table used has the maximum exciting force of 2.5 tons, frequency range of DC to 100Hz and accuracy of ±1.0%. An random wave from white noise with frequency of 5 to 40Hz and sinusoidal wave of 5 to 20Hz were applied as input, and acceleration amplitudes of 20 to 500gal were used depending on the purposes. Input and response waves recorded on magnetic tape recorders, were changed into real response waveforms through analog-digital conversion.

With regard to the random wave, the power spectra and cross spectra of responses were obtained and frequency response functions were calculated in corelation with the power spectra of the input wave, while phase differences were calculated from cross spectra. As for sinusoidal waveforms, the maximum response values, response ratios and phase differences were obtained.

(I) Head, Foundation Engineering Division, Public Works Research Institute, Ministry of Construction

RESULTS AND ANALYSES

The values of predominant frequencies of respective soils by the random wave were obtained from frequency response functions, as shown in Table 1. The response ratios of respective soils by sinusoidal wave were as shown in Table 2.

Liquefaction in Model 5 occurred at 500gal of the random wave and at 400gal with 10Hz sinusoidal wave. In model 6, liquefaction occurred at 200gal of the random wave and at 300gal with 10Hz sinusoidal wave. Running spectra were calculated every second for the response of the upper and lower layers in Model 5 and their ratios against the power spectra of input waves are shown in Fig. 6 in three dimensions. From the illustration, the transition of energy, the process of consumption and long liquefaction period can be understood.

The results of Models 7 to 9 are as shown in Table 3. Liquefaction occurred at 300gal in Model 7, 300gal in Model 8 and 200gal in Model 9 under 10Hz sinusoidal waves. From Table 3, since the respective elastic wave velocities are estimated as 28, 45 and 52m/sec, the apparent shearing stiffness rises with the increase of thickness. The pore water pressures at 300gal and 10Hz sinusoidal waves were P_1 = 10.8 in Model 7, P_1 = 9.3 and P_2 = 13.0 in Model 8, and P_1 = 11.3, P_2 = 11.5, P_3 = 12.8 and P_4 = 9.4g/cm^2 in Model 9. These show a trend that though the stiffness improves with the increase of sand layer thickness, the pore water pressure and response rate increase.

Table 4 shows the responses of accelerometers under random waves and table 5 shows maximum response values under sinusoidal waves with Models 9 and 10. From these, it can be known that pile responses are larger than soil responses, and that pile responses are approximately depending on the vibration of soils.

CONCLUSION

From these experiments, the followings were found.

1. The saturated sand layer on a cohesive soil is greatly subject to the influence of the vibratory energy accumulated and expanded in the cohesive soil.
2. Most of the vibratory energy can be estimated to have been converted into such work as breaking of sand layer and the kinetic energy of liquefied sand by the liquefaction of the saturated sand layer.
3. When the strength of the upper sand layer is high, the vibration of the lower soft soils is restrained and the vibration as a whole is reduced.
4. Since the weights of the upper sand layer and water has a great influence for the dynamic property of the lower soft soil, they cannot be neglected in analyses.
5. The existence of an impermeable layer on the saturated sand greatly affects liquefaction due to the reflection of vibration waves, the rise of pore water pressure of the sand layer below it, etc.
6. The effectiveness of stress for the prevention of liquefaction shall be related with the phenomenon that the coefficient of shearing stiffness of soils is improved.

7. The dynamic properties of piles in model soils are depending on the vibration of soils and amplified greatly at the liquefied sand layer.

ACKNOWLEDGEMENT

The author would like to thank Dr. Tatsuoka of the Univ. of Tokyo, Dr. Yanagisawa of Tohoku Univ. and Mr. Iwasaki of P.W.R.I. for their valuable advices to this experiment and Messrs. Mitsuie and Yamamoto of P.W.R.I. and Messrs. Tomozawa, Ukon and Onomura of Long Span Bridge Design Center for their assistance in the experiment.

Table 1 Predominant frequencies (Hz) in soils

Model No.	1	2	3	4	5	5'	6	6'
A2	10.9	24.1	11.1	21.5	20.0	23.2	18.0	20.5
A3	10.9	20.7	10.3	20.7	18.5	17.3	18.0	17.8
A4	10.9	24.1	9.6	21.1	18.5	17.3	18.0	19.0
A5	10.9	20.7	10.9	20.8	18.3	16.6	18.0	16.8
A6				20.9	18.0	16.3	18.0	17.5
A7				21.1	18.3	17.8	18.0	17.2

Note: 5 and 6 indicate values at 100gal input, 5', at 250gal and 6', at 300gal.

Table 2 Response rates in soils (at 10Hz)

Model No.	1	2	3	4	5	5'	6	6'
A2	2.7	1.7	2.7	1.3	1.5	0.8	1.4	0.5
A3	3.2	1.6	3.4	1.3	1.7	1.1	1.6	0.8
A4	2.0	1.1	2.4	1.3	1.5	1.1	1.5	0.9
A5	3.1	1.3	2.9	1.2	1.6	1.1	1.4	0.8
A6				1.4	2.0	0.9	1.7	0.5
A7				2.9	1.9	0.7	1.6	0.1

Note: 5' caused liquefaction at 10Hz and 400 gal
6' caused liquefaction at 10Hz and 300gal

Table 3 Influence given to the vibration properties of sand layer thickness

Name of accelerometer	Sand layer thickness 70cm (Model 9)		Sand layer thickness 50cm (Model 8)		Sand layer thickness 30cm (Model 7)	
	Predominant frequency	Response rate	Predominant frequency	Response rate	Predominant frequency	Response rate
A-2	18.8Hz	2.26	22.2Hz	2.08	-	-
A-3	19.1Hz	6.16	22.6Hz	5.42	24.0Hz	4.22
A-4	19.0Hz	8.60	22.6Hz	7.20	24.0Hz	4.72
A-5	19.0Hz	10.44				
A-6	19.0Hz	11.04				

Table 4 Predominant frequencies and response rates

Name of accelerometer	Model 10		Model 11	
	Predominant frequency	Response rate	Predominant frequency	Response rate
A-2	18.7Hz	4.52	18.6Hz	3.70
A-3	18.7	5.92	18.6	5.20
A-4	18.7	5.54	18.6	5.14
A-5	18.7	9.24	18.6	8.00
A-6	18.5	4.73	18.6	4.31
A-7	18.7	5.02	18.6	5.16
A-8	18.6	6.76	18.6	6.18

Table 5 Maximum response values with sinusoidal waves applied

Model / Input / Appa-ratus	Model 10			Model 11		
	10Hz 200gal	10Hz 300gal	10Hz 400gal	10Hz 200gal	10Hz 300gal	10Hz 400gal
A-1	211.2gal	317.0gal	481.9gal	194.0gal	320.1gal	448.0gal
A-2	489.5	684.4	996.1	337.7	586.8	779.2
A-3	367.7	548.2	818.0	360.4	627.6	822.0
A-4	357.0	537.0	882.8	311.1	635.0	828.1
A-5	1,034.4	1,174.1	3,520.4	882.9	2,141.1	3,393.9
A-6	458.5	503.0	788.0	326.1	560.7	814.5
A-7	311.5	497.9	797.0	317.8	551.0	768.3
A-8	617.4	906.1	1,270.1	582.0	823.6	980.5

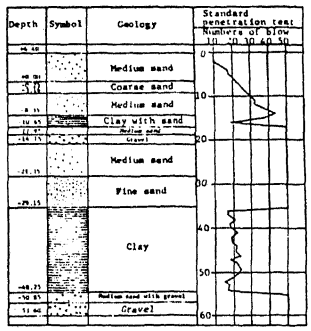

Fig. 1 Example of geologic features of Fukui Basin

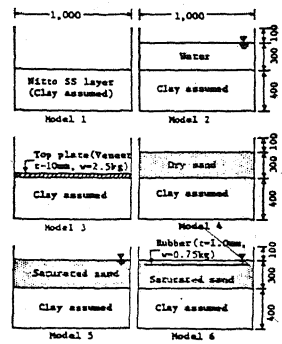

Fig. 2 Kinds of models

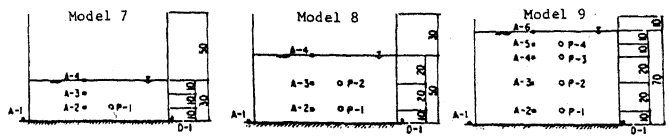

Fig. 3 Arrangement of measuring apparatuses in Models 7, 8 and 9

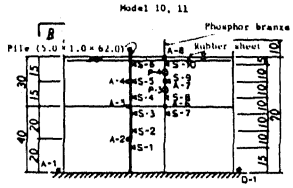

Fig. 4 Arrangement of measuring apparatuses in Models 10 and 11

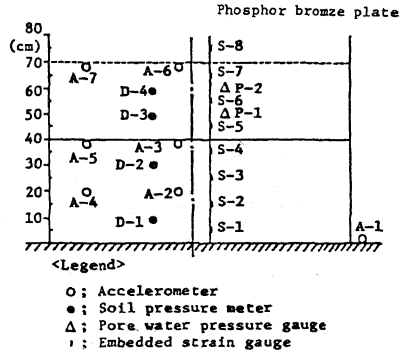

Fig. 5 Arrangement of measuring apparatuses

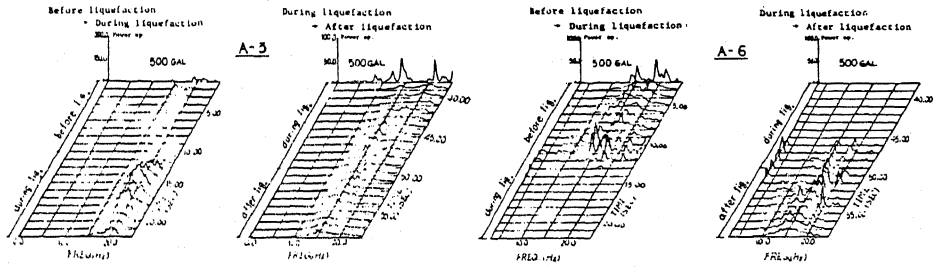

Fig. 6 Acceleration power spectrum ratios of upper and lower soil layers before and after liquefaction